7-6 Development of Epitaxial NbN THz Mixers

KAWAKAMI Akira, TAKEDA Masanori, and WANG Zhen

We have developed fabrication processes for epitaxial NbN/MgO/NbN trilayers. The surface resistance of the epitaxial NbN films was estimated to be approximately $2.6-25\,m\Omega$ at $0.1-0.8$ THz. We also have succeeded to fabricate epitaxial NbN/MgO/NbN Josephson tunnel junctions with good tunneling characteristics. The fully epitaxial SIS mixers showed low-noise properties over the Nb gap frequency, and the DSB receiver noise was 260 K at 795 GHz. We also report on a new structure and the new process of HEB mixers that uses fluoride radical etching to improve both durability and reproducibility. The receiver noise temperature of the HEB mixer was evaluated and it was about 615 K at 780 GHz.

1 Introduction

In the fields of next generation ultra-high-speed communications, earth environment observation, and radio astronomy, the development of THz receivers and oscillators is eagerly anticipated. To succeed, the conductor materials that constitute these devices must have low-loss characteristics. With conventional superconductor materials based on niobium (Nb), the gap frequency (f_g) is approximately 725 GHz. This material is therefore unsuitable as conductor material in the THz range, which lies above this gap frequency. Niobium nitride (NbN; f_g = 1.4 THz) has a higher gap frequency than Nb and has been proposed as a superconductor material to replace Nb. However, it is known that the low-loss characteristics of NbN depend significantly on the crystallinity of the grown film[1]. Accordingly, to develop THz NbN devices, fabrication processes maintaining high-crystallinity were needed. This requirement poses a difficult challenge in the development of an NbN-based device.

We can epitaxially grow a single layer of NbN film using single-crystal substrates with high lattice matching, such as magnesium oxide (MgO)[2][3]. However, in order to construct a receiver or an oscillator, we will have to construct the tuning and matching circuits using microstrip lines composed of low-loss thin films. Figure 1 shows a schematic diagram of these microstrip lines. To fabricate the tuning and matching circuits, we must grow a dielectric layer on the epitaxial NbN single-layer film and then deposit the NbN film on the dielectric layer, continuing to maintain the requisite high crystallinity. Low-loss, low-dielectric-constant silicon oxides (SiO and SiO_2) have often been used as the dielectric material. However, these materials feature large lattice mismatch with NbN, and NbN deposited directly on SiO or SiO_2 forms a polycrystalline film. Thus, the superconductivity transition temperature (T_C) decreases and resistivity increases with this combination of materials, probably due to the grain boundaries present in the film, leading to extremely large conductor loss in the THz frequency
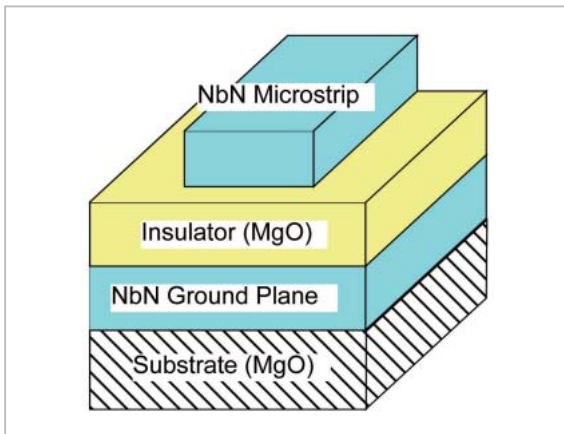
Fig.1 *Schematic diagram of microstrip line*

range[1].

In recent years, some research institutions have investigated a potential solution in the use of NbTiN. This material displays a relatively high T_C and low resistivity, even in the form of a polycrystalline film ($T_C = 15.2$ K, resistivity at 20 K of $\rho_{20K} = 75 \, \mu\Omega$ cm, $fg = 1.2$ THz). Various SIS mixers with NbTiN matching circuits have been reported to produce relatively satisfactory results[4]-[6]. However, T_C and ρ_{20K}, which determine the superconductivity conductor loss, are both better for an epitaxially grown NbN film (T_C of approximately 16 K, ρ_{20K} of approximately $60 \, \mu\Omega$ cm). In other words, if we can epitaxially grow all layers constituting the device — including NbN and dielectric films — we can expect higher performance and operation at higher frequencies than with devices constructed using NbTiN. With these issues in mind, we are using MgO, which shows high lattice matching with NbN, as the dielectric material in an attempt to fabricate NbN THz devices in which all layers constituting the device are epitaxially grown.

An RF sputtering technique that uses a sintered MgO target (the "RF-MgO" technique) has frequently been reported in references as a technique for depositing an MgO film[7][8]. We also tried to fabricate an NbN/MgO bilayer film using RF-MgO. However, even when we used an MgO single-crystal substrate, which provides the ideal conditions for MgO film deposition, to grow the several hundred nanometers of RF-MgO required to fabricate a mixer, the superconductivity performance (T_C, ρ_{20K}) of the NbN film grown on the RF-MgO film was markedly lower than those of an epitaxial NbN film directly deposited on an MgO single crystal substrate. We concluded that epitaxial growth is difficult with an RF-MgO film. Regarding the possible causes of this problem, we infer that the low deposition rate of the RF sputter technique and surface heating due to the ion bombardment associated with film deposition led to the formation of a columnar structure in the MgO film. As a result, grain boundaries are formed in the NbN film fabricated on the MgO film, resulting in a decrease in T_C and an increase in resistivity. Based on this supposition, we attempted to fabricate an MgO film based on the DC reactive sputtering technique that uses a metal Mg target (the "DC-MgO" technique)[9][10]. With film deposition based on DC reactive sputtering, the electrode potential is not reversed during deposition, and thus the effects of ion bombardment and surface heating of the sample are presumably less than in RF sputtering. With this method, we succeeded in epitaxial growth of an NbN/MgO/NbN trilayer film, enabling the fabrication of a fully epitaxial NbN/MgO/NbN-SIS junction[11]-[13].

This paper describes the unique epitaxial NbN/MgO device fabrication technique developed by NICT and shows how the epitaxial NbN film is a superior low-loss material in the sub-millimeter range. We also clarify the low-noise properties of a prototype quasi-optical SIS mixer, which we built using the epitaxial NbN/MgO/NbN-SIS junction, operating at 795 GHz. This paper also presents a discussion of a hot electron bolometer (HEB) that is expected to operate with extremely low noise at frequencies higher than the NbN gap frequency (1.4 THz). We propose a unique fabrication process to improve mechanical and electronic durability and the reproducibility of device characteristics, evaluate these characteristics, and discuss its possibilities as a THz mixer.

2 Epitaxial NbN/MgO/NbN-SIS mixer in THz range

An SIS junction consisting of a superconductor (S) / insulator (I) / superconductor (S) sandwich structure has strong non-linear characteristics that render it difficult to implement with semiconductor devices. Today, SIS mixers that make use of this nonlinearity show ultra-low-noise properties close to the quantum noise limit in the millimeter and sub-millimeter ranges and are already widely used in the fields of earth environment observation and radio astronomy. The SIS junction displays high junction capacitance due to its structure and essentially requires a tuning circuit in order to eliminate the capacitance component in mixer operation. However, the required operating frequencies employed in recent years have exceeded the gap frequency (725 GHz) of the Nb used in constructing SIS mixers, and the degradation in performance of the tuning circuit associated with the increase in Nb conductor loss has come to pose a significant problem. With these circumstances in mind, we developed a technique of device fabrication based on epitaxial NbN, which is expected to provide superior low-loss characteristics in the frequency range up to 1.4 THz. Here, we discuss the possibilities of a THz mixer based on an epitaxial NbN/MgO/NbN-SIS junction.

2.1 Evaluation of DC and high-frequency characteristics of epitaxial NbN/MgO/NbN trilayer film
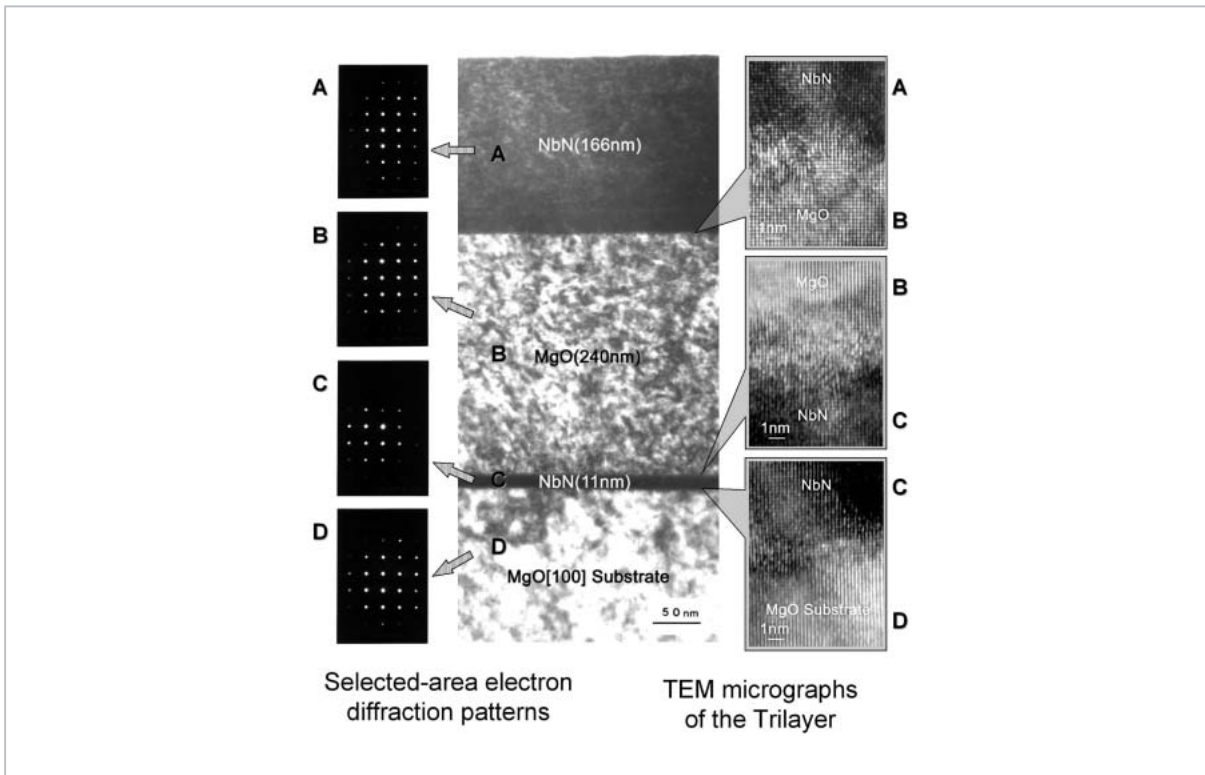
Figure 2 shows the X-ray diffraction patterns of the NbN/MgO/NbN trilayer film and the NbN single-layer film. We describe the details of the fabrication of the trilayer film in reference[11]. In the trilayer film (a), the RF-MgO (film thickness of 1.3 nm) on the lower NbN film is an antioxidant film to protect the lower NbN film surface against the oxygen used as the discharge gas in DC-MgO film deposition. The lower NbN film (11 nm) is made thinner than the upper NbN film
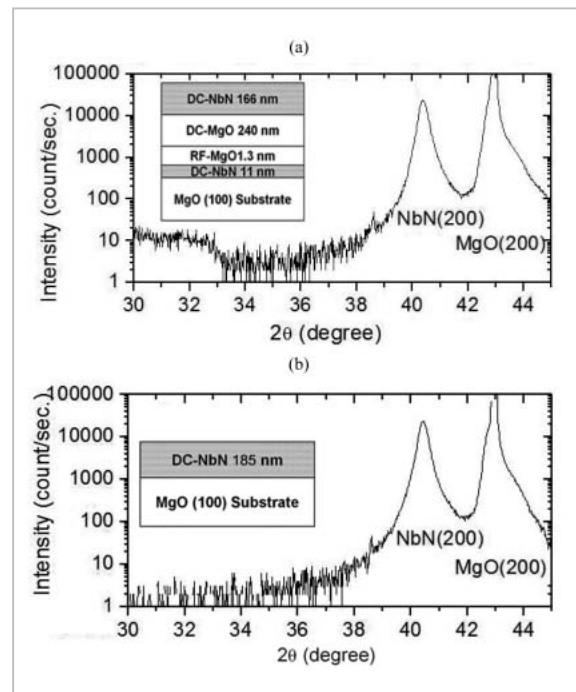
(166 nm) to ensure that the diffraction peaks from the upper NbN film are dominant among all peaks in X-ray analysis. The NbN (200) peak in the X-ray diffraction pattern [Fig. 2 (a)] of the trilayer film does not differ from that in the diffraction pattern [Fig. 2 (b)] for the NbN film directly deposited on the MgO single-crystal substrate. The DC superconductivity characteristics, T_C and ρ_{20K}, of the upper NbN film are 15.8 K and 57.4 $\mu\Omega$ cm, respectively. These values do not indicate degradation compared with the values for the NbN film directly deposited on the MgO single-crystal substrate ($T_C = 15.6$ K, $\rho_{20K} = 64$ $\mu\Omega$ cm), attesting to the satisfactory performance of the trilayer film.
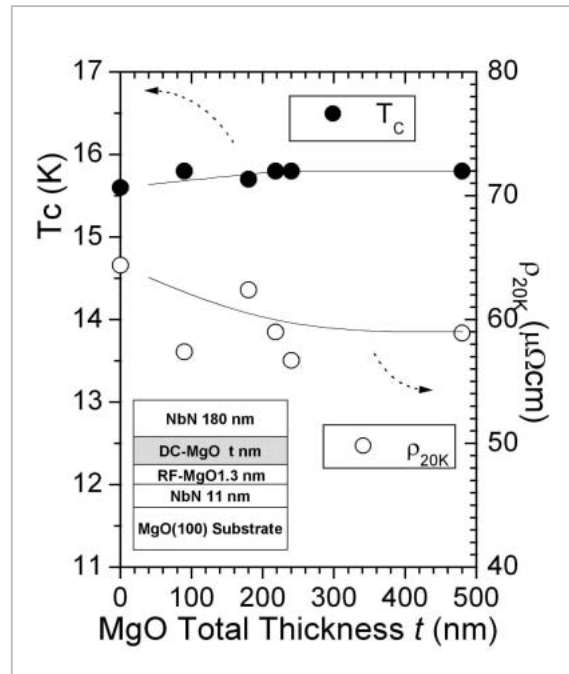
Next, we performed high-resolution TEM observation of this trilayer film. Figure 3 shows an electron diffraction image and cross-sectional TEM image of each layer. The electron diffraction images all show similar clear electron diffraction lattice spots with cubic distributions, which indicates that each layer is grown in the same direction as the substrate. The TEM lattice images of the interfaces between the layers also do not show amor-

phous layers, confirming growth in a single direction. The approximately 1-μm TEM observation area does not show any signs of columnar structures in the trilayer film. The X-ray analysis and the above results indicate that the NbN/MgO/NbN trilayer film is epitaxially grown.

Figure 4 shows the dependence of the superconductivity characteristics of the upper NbN film on the thickness of the interlayer MgO film in the epitaxial NbN/MgO/NbN trilayer film. Here, we varied the film thickness of the interlayer MgO film between 0 nm and 480 nm. The transition temperature, T_C, and ρ_{20K} of the upper NbN film were unchanged from those of the NbN film directly deposited on the MgO single-crystal substrate and showed no degradation. Even with an interlayer MgO film thickness of 480 nm, the upper NbN film showed superior DC characteristics, at approximately 15.8 K and 59.0 $\mu\Omega$ cm. These T_C and ρ_{20K} values are both better than those obtained with the NbTiN film previously used in the tuning circuit of the SIS receiver, which already provided satisfactory results.

The BCS theory, used to express superconductivity characteristics, indicates that the epitaxial NbN/MgO/NbN trilayer film will reveal

superior low-loss characteristics in the THz range up to 1.4 THz, which is the gap frequency of NbN.

In the past, we improved the operating frequency of the SIS mixer by increasing the critical current density of the SIS tunnel junction and by minimizing the junction capacitance by minimizing the junction area. However, the maximum critical current density that we can now obtain while maintaining satisfactory nonlinearity is approximately 20 kA/cm^2 in the NbN/MgO/NbN tunnel junction we have previously reported[13]. The degradation of characteristics associated with the increase in J_C has also been reported in the Nb-based junction[14][15]. These reports indicate that inevitably we must use an SIS junction with a high junction capacitance in the development of an SIS mixer in the THz range. We conclude as a result that, in the conductor material that will constitute the circuits (including the tuning circuit), we must obtain low-loss characteristics superior to those of conventional materials. Thus, we attempted to evaluate the surface resistance, R_S, of the epitaxial NbN/MgO/NbN trilayer film in the sub-millimeter range.

We fabricated a cavity-integrated Josephson junction, in which this junction is placed in the middle of a microstrip cavity, and attempted to evaluate the surface resistance of the epitaxial NbN film in the sub-millimeter range. Figure 5 shows a photograph of our fabricated cavity-integrated Josephson junction device. The Josephson junction here is fully epitaxially grown. This component serves as a superconducting two-terminal device and operates as a voltage dependent oscillator in the sub-millimeter range due to the AC Josephson effect. Accordingly, the Josephson junction placed in the cavity generates resonance steps due to its current-voltage characteristics, for voltage values at which the self-oscillating frequency agrees with the resonance frequency[16]. As the height of these steps depends on the cavity loss, we determined the cavity loss by comparing the measured values and the results of computer simu-

lations and derived the surface resistance of the NbN film that constitutes the cavity. We describe the details of the evaluation method in reference[17]. Figure 6 shows the surface resistance, R_S, of the epitaxial NbN film in the sub-millimeter range. The solid, dotted, and broken lines in the figure correspond to the theoretical values for NbN, Nb, and Al, respectively. The surface resistance of the NbN film in the frequency range of 0.2 THz to 0.8 THz is approximately 3.5 mΩ to 25 mΩ which is lower than the theoretical value for Al. Here, J. Zmuidzinas et al.[18] investigated the approximate magnitude of the surface resistance, R_S, required for the conductor material constituting the tuning circuit as follows. The surface reactance, X_S, of the superconductor is expressed as $X_S = \omega L = \omega \mu_0 \lambda$. In the equation, λ is the wavelength of the superconducting magnetic penetration depth and μ_0 is the permeability of a vacuum. When
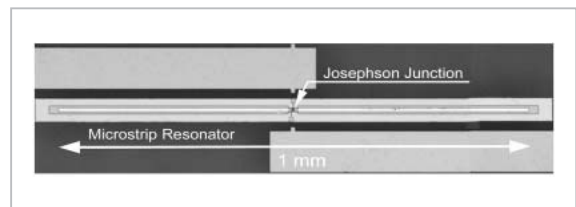
Fig.5 Photograph of cavity-integrated Josephson junction device for evaluating NbN surface resistance
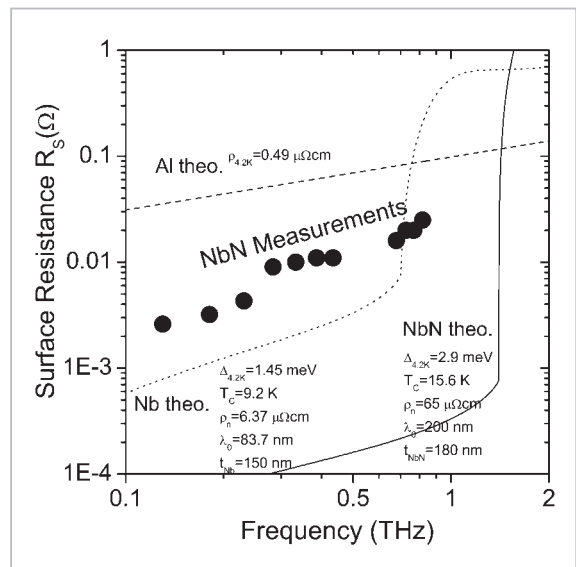
Fig.6 Surface resistance of epitaxial NbN film in submillimeter range

one constructs the tuning circuit with microstrip lines, at least the surface resistance, R_s, needs to be sufficiently smaller than X_s. When the effects of the junction capacitance, C_J, at the design frequency are considered, the surface resistance of the conductor material constituting the tuning circuit needs to satisfy the expression below.

$$R_s \ll 2\pi\eta_0\lambda / (\lambda_0 Q) \qquad (1)$$

Here, $\eta_0 = 377\ \Omega$, and λ_0 is the wavelength in free space. Q is defined as $Q = \omega C_J R_N$ with a normal resistance R_N of the SIS junction and a junction capacitance C_J; this parameter reflects the bandwidth of the SIS mixer. Here, if we assume typical values for the parameters, namely, the product of the junction resistance and the area as $R_N A = 20\ \Omega\,\mu m^2$, $C_J/A = 120\ fF/\mu m^2$, $f = 0.8$ THz, and $\lambda = 200$ nm, we obtain $R_s \ll 0.11\,\Omega$ from Expression (1). On the other hand, the measured value of the surface resistance of NbN is approximately $25\ m\Omega$ near 0.8 THz. Thus, the epitaxial NbN/MgO/NbN trilayer film is considered effective as a conductor material constituting the THz SIS receiver.

2.2 870-GHz quasi-optical SIS receiver based on epitaxial NbN/MgO/NbN tunnel junction

Nonlinearity in the tunnel junction significantly influences receiver performance. We investigated the fabrication processes of the epitaxial NbN/MgO/NbN tunnel junction using an MgO tunnel barrier and attempted to fabricate a tunnel junction fully epitaxially grown, including the interlayer insulating film[13]. The NbN/MgO/NbN tunnel junction is fabricated on an MgO (100) single-crystal substrate. The NbN film is deposited by the DC reactive sputtering technique. The MgO film, which serves as the tunnel barrier, is deposited by the RF sputtering technique. Here, the substrate is not heated during deposition. We confirmed by X-ray diffraction that the fabricated NbN/MgO/NbN trilayer film is epitaxially grown. The superconductor charac-

teristics of the NbN films show the satisfactory values of $T_C = 15.7$ K and $\rho_{20K} = 57\ \mu\Omega cm$ for both upper and lower electrodes.

Figure 7 shows the current-voltage characteristics of typical epitaxial NbN/MgO/NbN-SIS junctions at 4.2 K. Here, R_N is the junction resistance at 8 mV. With the junction resistance at 4 mV, R_{4mV}, and the critical current, I_C, we have defined the product, $V_m = I_C R_{4mV}$, as a parameter indicating the leak
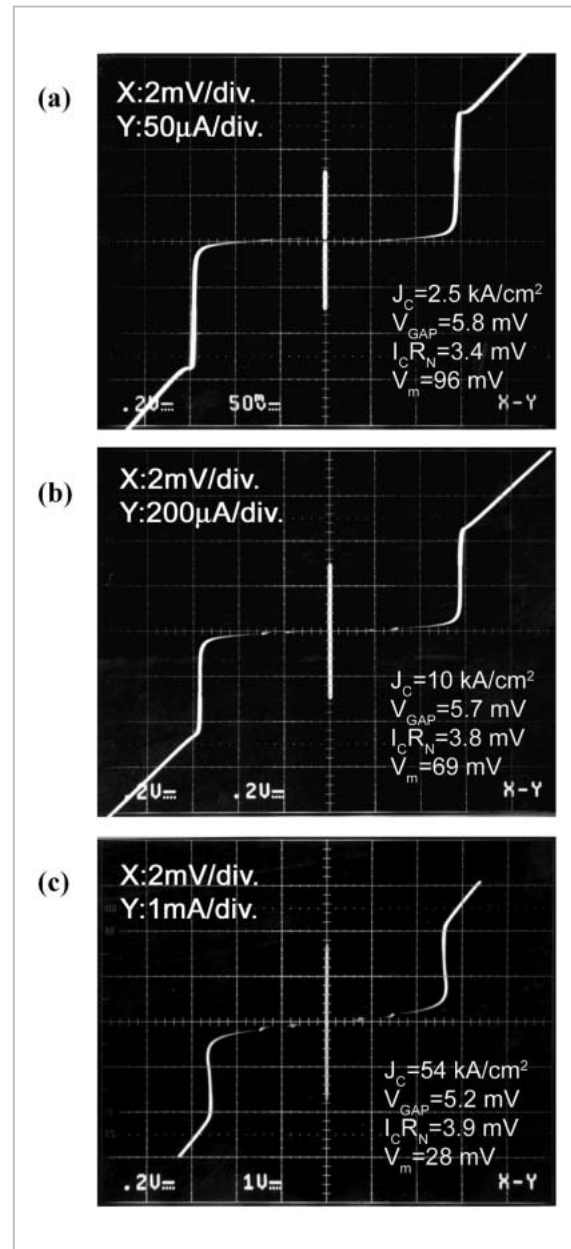

Fig.7 Current-voltage characteristics of epitaxial NbN/MgO/NbN-SIS junction at 4.2 K. Junction critical current density: $J_C = 2.5\,kA/cm^2$ (a), $10\,kA/cm^2$ (b), and $54\,kA/cm^2$ (c)

current. Each junction is approximately 3.1 μm^2, and the critical current density of the junction, J_C, is 2.5 kA/cm^2(a), 10 kA/cm^2(b), and 54 kA/cm^2(c). In both cases (a) and (b), we obtained satisfactory tunneling characteristics with high gap voltage and low leak current values. Also in the case of 54 kA/cm^2, which has a high J_C value, we conclude that the tunneling characteristics we obtained were satisfactory, with $V_m = 28$ mV, although self-heating decreases V_{GAP}.

We built a prototype quasi-optical NbN/MgO/NbN-SIS receiver composed of the epitaxial trilayer film and evaluated its characteristics[19]. Figure 8 shows a photograph of our fabricated receiver device. For the tuning circuit, we used a tuning method that makes the epitaxial NbN-SIS junction itself function as an all-wavelength cavity, to remove the imaginary components caused by junction capacitance. The dimensions of the junction are 7 μm long and approximately 0.6 μm wide, and the design frequency is 870 GHz. The junction couples with the space via a twin-slot antenna, and the antenna and the junction are connected with a 2-μm-wide 1/4-wavelength NbN/MgO/NbN microstrip matching circuit via a coplanar line matched with the antenna impedance. These components are fabricated on the MgO (100) single-crystal substrate, and we confirmed by X-ray diffraction that all of the NbN and MgO films constituting the receiver were epitaxially grown.

We evaluated the receiver performance using a quasi-optical receiver system. We describe the details of the configuration of the measurement system in reference[20]. Figure 9 shows the sub-millimeter response characteristics of the fabricated SIS receiver. We irradiated electromagnetic waves at a frequency of 795 GHz and evaluated the receiver noise temperature based on the Y-factor method using thermal radiation at 77 K and 295 K. The dotted line in the figure indicates the IF output power corresponding to thermal radiation at 77 K, and the solid line indicates the IF output power corresponding to thermal radiation at 295 K. We observed clear photon-
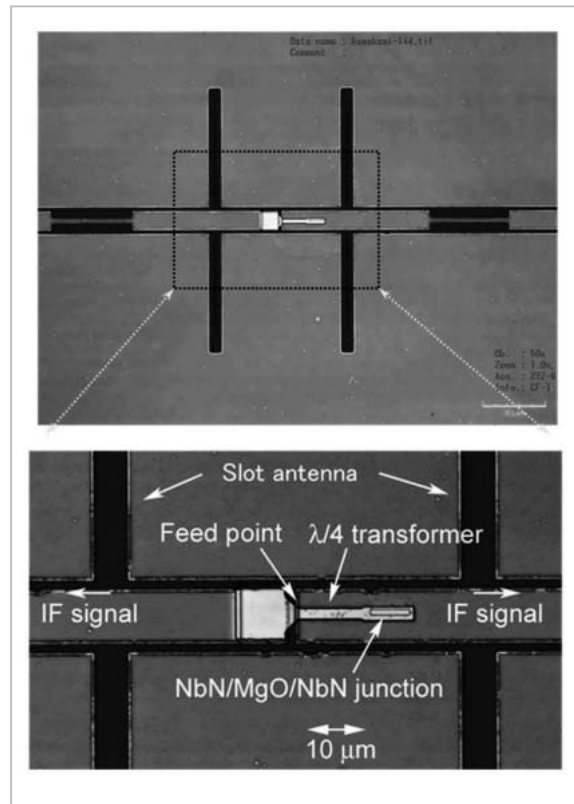
Fig.8 Microscope image of 870-GHz quasi-optical SIS electromagnetic wave receiver
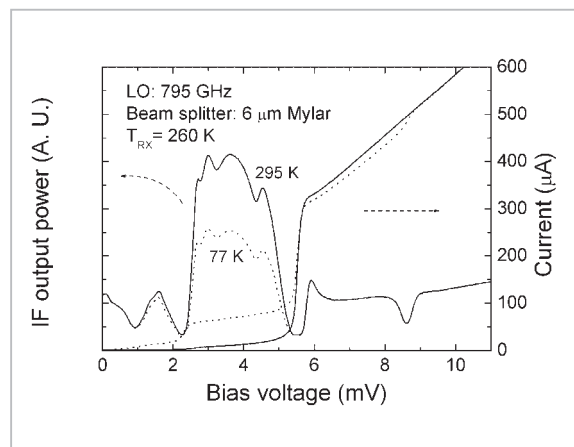
Fig.9 Electromagnetic wave response characteristics of NbN/MgO/NbN-SIS receiver under irradiation of submillimeter waves

assisted tunneling steps associated with the LO irradiation. In this experiment, the critical current density, J_C, of the tunnel junction was approximately 4 kA/cm^2, which differs significantly from the design value (25 kA/cm^2), and the $\omega C_J R_N$ product was approximately 50. However, the SIS receiver showed a low noise

characteristic, with a receiver noise temperature of $T_{N(DSB)} = 260$ K. This result indicates that the epitaxial NbN/MgO/NbN trilayer film used in the matching circuit features ultra-low-loss characteristics. We thus conclude that the epitaxial NbN/MgO/NbN-SIS receiver is a promising prospective THz SIS receiver.

3 Study of THz NbN-HEB

The SIS mixer is the best low-noise, high-sensitivity heterodyne detector in the millimeter and sub-millimeter ranges currently available. However, as discussed earlier, the SIS mixer structurally incorporates high parasitic capacitance and thus requires a tuning circuit. Nevertheless, when we construct a tuning circuit with microstrip lines, the characteristics of the materials constituting the circuit determine the upper limit frequency of the mixer performance. Even when we use NbN, it is presumably difficult to achieve a satisfactory performance at or above 1.4 THz. In the THz frequency range at or above 1.4 Hz, HEB has raised expectations as a potential low-noise mixer as structurally it displays low parasitic capacitance and does not require a tuning circuit.

3.1 Consideration of fabrication process of NbN-HEB by fluoride radical etching

HEB, which has become the focus of expectations as a low-noise mixer in the THz range, features a structure consisting of an extremely thin superconductor film of several nanometers placed between close-set metal electrodes. We have already succeeded in fabricating and evaluating an HEB mixer (IF bandwidth of 2.0 GHz and noise temperature of 780 K at 900 GHz) offering superior receiving performance with this process[21]. However, the fabricated HEB has low mechanical and electrical durability, representing an obstacle in practical applications. Figure 10(a) shows a schematic diagram of a cross-section of the HEB constructed through a conventional device-fabrication process. In
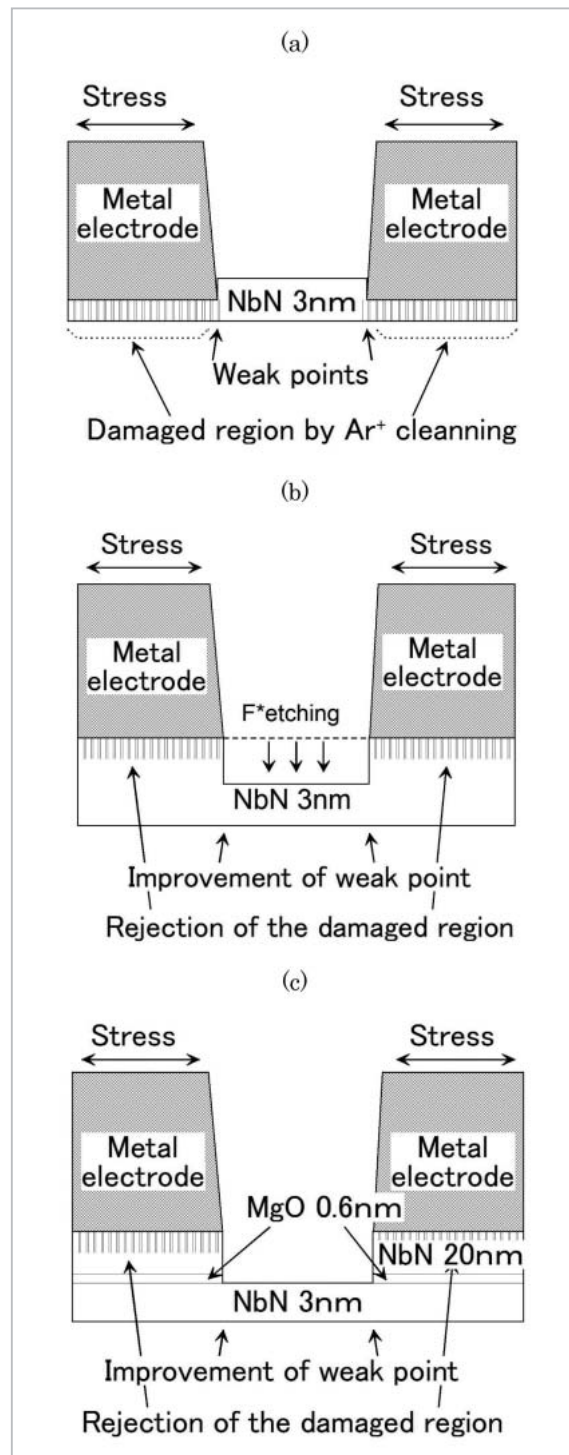

Fig.10 Schematic diagram of cross-section of HEB. (a) device structure by conventional process, (b) device structure for improving durability, and (c) device structure by new process

this conventional process, metal electrodes are deposited on an ultra-thin superconducting film approximately 3-nm thick. Here, the NbN ultra-thin film probably becomes thinner

through the NbN surface cleaning (including Ar ion beam cleaning) performed when the metal electrodes are attached. This increases the probability of damaging the device through external surges. In addition, the thermal cycles due to cooling at the temperature of liquid helium (4.2 K) and the stress in the metal electrodes may mechanically break the thinned NbN film.

As a measure to prevent these problems, we are considering the device structure indicated in Fig. 10(b). First, a relatively thick NbN film of several tens of nanometers is deposited, instead of the approximately 3-nm ultra-thin NbN film. The metal electrodes are then attached. Finally, the NbN film is etched to the appropriate thickness of 3 nm by fluoride radical etching to complete the HEB device structure. This method ensures that the NbN film does not contain areas thinner than 3 nm and is assumed to increase mechanical and electrical strength as a result. Further, we also conclude that degradation of superconductivity by Ar ion cleaning can be eliminated by maintaining the initial thickness of the NbN film at approximately several tens of nanometers. However, it is difficult to determine the thickness of an NbN strip with the structure shown in Fig. 10(b). Thus in this study we adopted the device structure indicated in Fig. 10(c). With this structure, the inter-layer MgO film is extremely thin, at 0.6 nm, such that the current density of the tunnel current is high (approximately 20 kA/cm^2 or more). As a result, we assume that we can ignore electrical effects with respect to the film.

To realize the new process, an etching technique is required that will etch the NbN film without damaging it. Thus, we developed a new fluoride radical etching technique. Figure 11 shows a schematic diagram of the developed technique. Here, we used an ECR (Electron Cyclotron Resonance) ion source as the source of the fluorine radicals. CF$_4$ gas is introduced into the ECR ion source to generate plasma. In ordinary ion beam etching, the ions are extracted using a grid applied with a
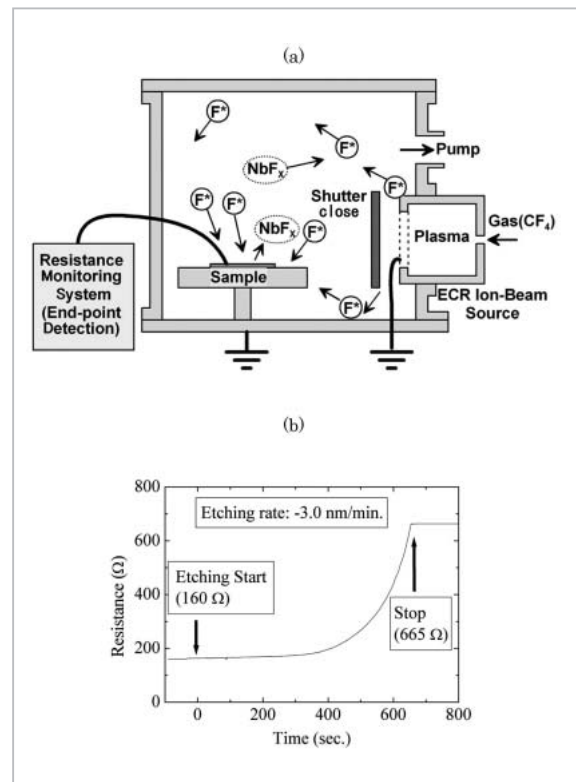
Fig.11 Fluoride radical etching technique. (a) schematic diagram and (b) time variation of film resistance measured

DC voltage that accelerates the CF$_3^+$ ions, which are emitted to the sample for etching. Here, the ion extraction grid is set at 0 V and the fluorine radicals are diffused by the concentration distribution only. The fluorine radicals that reach the NbN film surface react with Nb and contribute to the etching. Etching with neutral fluorine radicals instead of fluoride ions involving electric acceleration suppresses the degradation of the ultra-thin film characteristics by ion bombardment.

We fabricated a four-terminal pattern on the sample in advance to gauge the resistance and enable measurement of the film thickness. Using electrically neutral fluorine radicals makes it possible to measure the film resistance during etching. Measuring this resistance in turn can provide information on the approximate amount of remaining NbN film to be etched. Figure 11(b) shows the time variation of the measured film resistance. In this experiment, the film resistance was 166 Ω (film thickness of 20 nm) when etching began.

Approximately 11 minutes later, the film resistance increased to 665 Ω due to the fluoride radical etching. If we assume a constant resistivity for the NbN film, the thickness of the remaining film is estimated as 4.8 nm based on the final resistance value. However, when we measured the thickness using a contact-stylus-type surface profiler (Alpha-Step 500: produced by KLA-Tencor Corp.; vertical resolution: 0.1 nm), the thickness was 5.4 nm. Considering that the resistivity increases during the first stage of film growth, we believe that these film thickness values are satisfactory. The superconductor transition temperature, T_C, and the resistivity at 20 K, ρ_{20K}, for the ultra-thin-film after fluoride radical etching are $T_C = 11.3$ K and $\rho_{20K} = 92\,\mu\Omega\,cm$, respectively. These values are equivalent to those of NbN ultra-thin film ($T_C = 12.8$ K and $\rho_{20K} = 110\,\mu\Omega\,cm$ when the film thickness is 5.5 nm) directly deposited on the MgO single-crystal substrate. These results show that the etching does not damage the film.

## 3.2 Response of epitaxial NbN-HEB to electromagnetic waves

Figure 12 shows a microscope image of the HEB fabricated using the fluoride radical etching technique. The HEB consists of an NbN strip, tungsten (W) electrodes, and a log periodic antenna made of an Al film. First, we deposited the three layers of NbN (20 nm), MgO (0.6 nm), and NbN (3 nm) on the MgO (100) single-crystal substrate. Next, we fabricated the W electrodes and the Al antenna. We then etched the upper NbN (20 nm) of the tri-layer film by fluoride radical etching to form the strip. Here, we confirmed that the NbN and MgO films are epitaxially grown. Because the current density in the strip increases as the size of the device decreases, we adopted tungsten for the electrode material, as tungsten has relatively low resistivity and a high melting point. The NbN strip is fabricated by the electron beam lithography technique, and its dimensions are 3.0 nm thick, 2.5 μm wide, and 0.5 μm long.

We evaluated the durability of our fabricated HEB device. After we repeated 14 thermal cycles between room temperature and 4.2 K over the course of 50 days while attaching and detaching the terminals of the HEB device, the DC characteristics had not changed. We conclude accordingly that the new process has led to improved electrical and mechanical durability. Figure 13 shows the response of the HEB mixer to electromagnetic waves at 780 GHz. We evaluated the receiver noise temperature using the Y-factor method. Our results indicated successful achievement of low noise, with a receiver noise temperature of $T_{N(DSB)} = 615$ K at a measurement frequency of 780 GHz.
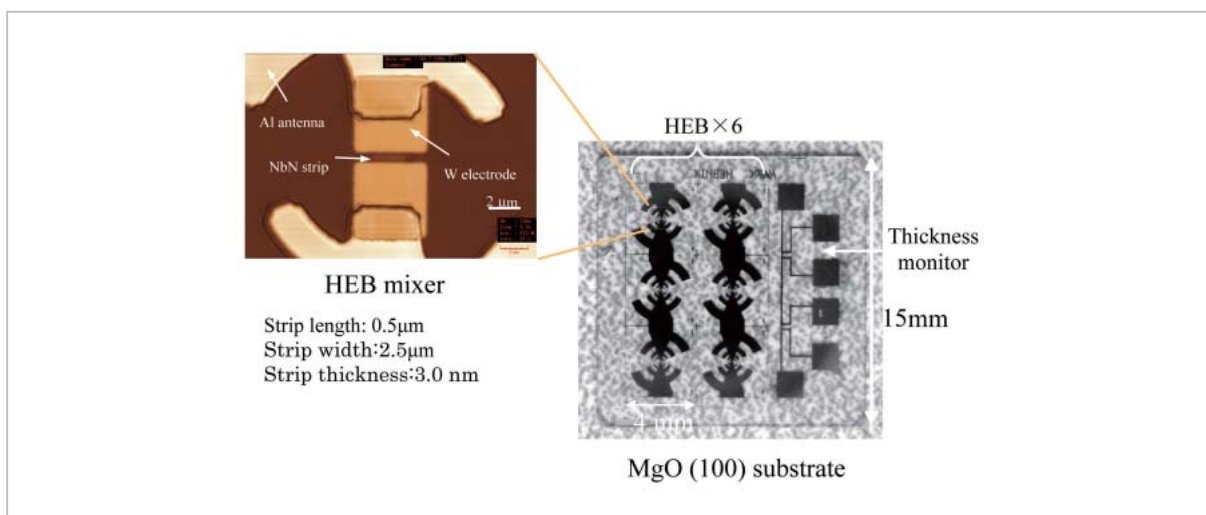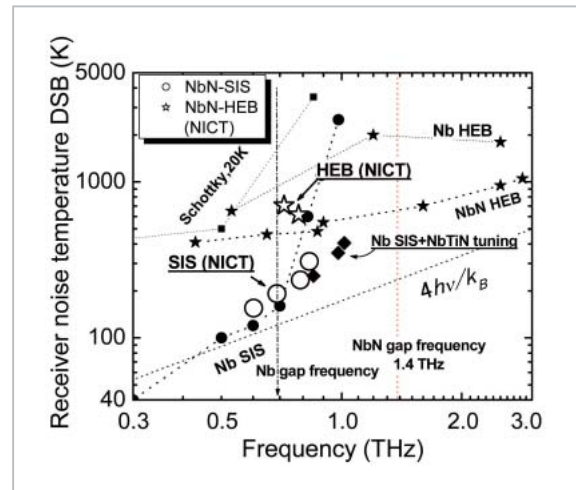

Fig.12 *Microscope image of HEB*
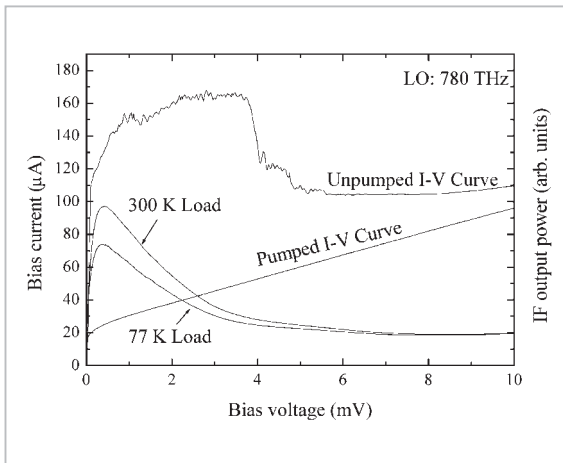
Fig.13 *Electromagnetic wave response characteristics of HEB mixer under irradiation of submillimeter wave*

Fig.14 *Receiver noise temperature of various terahertz mixers*

4 Conclusions

To develop a low-noise mixer in the THz range, we investigated an epitaxial NbN/MgO/NbN device fabrication technique. We evaluated the T_C and ρ_{20K} of the upper NbN film of an epitaxial NbN/MgO/NbN tri-layer film. Our results indicated no degradation of superconductivity associated with an increase in the thickness of the interlayer MgO film, and all samples showed satisfactory DC characteristics at approximately 15.7 K and $60\,\mu\Omega\,cm$. The NbN film fabricated showed superior low-loss characteristics for the frequency range from 0.2 THz to 0.8 THz with a surface resistance of approximately 3.5 mΩ to 25 mΩ.

The epitaxial NbN/MgO/NbN-SIS junctions that we fabricated all showed satisfactory tunneling characteristics with high gap-voltage and low leak-current values. The prototype quasi-optical SIS mixer showed superior low-noise characteristics, with a receiver noise temperature of 260 K (DSB) at 795 GHz.

To improve the durability and reproducibility of the HEB characteristics, we proposed a new HEB fabrication process based on fluoride radical etching. The characteristics of the HEB device we fabricated did not change after 14 thermal cycles over the course of 50 days. We conclude that device durability has improved accordingly. We also evaluated the receiver noise temperature of the HEB mixer and confirmed low noise of 615 K (DSB) at 780 GHz.

Figure 14 shows the noise temperature of the diverse heterodyne receivers presently reported as in use for the frequency range from 0.3 THz to 3 THz. Another research institution has now reported on a superior Nb-SIS mixer that uses NbTiN in the tuning circuit near 1 THz. The figure also shows that the NbN/MgO/NbN-SIS of NICT features equivalently low noise. Here, the gap frequency of NbTiN is 1.2 THz. We conclude that the epitaxial NbN-SIS mixer is a promising prospective ultra-low-noise receiver in the frequency range up to 1.4 THz, if we optimize the tuning and matching circuits (including the antenna). On the other hand, although the HEB features lower noise than the NbN-SIS mixer near 1 THz, it does not display frequency dependency, as indicated in other reports. Thus, we conclude that we can expect low-noise operation in the frequency range of several THz.

Acknowledgement

References

1 Y. Uzawa, Z. Wang, and A. Kawakami, "Terahertz NbN/AlN/NbN mixers with Al/SiO/NbN microstrip tuning circuits", Proc. 9th Int. Symp. on Space THz Technology, Pasadena, CA, pp.273-281, Mar. 1998.

2 Z. Wang, A. Kawakami, Y. Uzawa, and B. Komiyama, "Superconducting properties and crystal structures of single-crystal niobium nitride thin films deposited at ambient substrate temperature", J. Appl. Phys., Vol.79, No.10, pp.7837-7842, May 1996.

3 A. Shoji, "Fabrication of All-NbN Josephson tunnel junctions using single crystal NbN films for the base electrodes", IEEE Trans. Magn., Vol.27, pp.3184-3187, Mar. 1991.

4 J. Kawamura, J. Chen, D. Miller, J. Kooi, J. Zmuidzinas, B. Bumble, H. G. LeDuc, and J. A.Stern, "Low-noise submillimeter-wave NbTiN superconducting tunnel junction mixers", Appl. Phys. Lett., Vol.75, pp.4013-4015, Dec. 1999.

5 J. A. Stern, B. Bumble, H. G. LeDuc, J. W. Kooi, J. Zmuidzinas, "Fabrication and DC-characterization of NbTiN based SIS mixers for the use between 600 and 1200 GHz", Proc. 9th Int. Symp. on Space THz Technology, Pasadena, CA, pp.305-313, Mar. 1998.

6 B. D. Jackson, A. M. Baryshev, G. de Lange, J. R. Gao, S. V. Shitov, N. N. Iosad, and T. M. Klapwijk, "Low-noise 1 THz superconductor-insulator-superconductor mixer incorporating a NbTiN/SiO2/Al tuning circuit", Appl. Phys. Lett., Vol.79, pp.436-438, Jul. 2001.

7 S. Nagaoka, K. Hamasaki, T. Yamashita, and T. Komata, "Microstructure and superconductivity in epitaxial MgO/NbN multilayers", Jpn. J. Appl. Phys., Vol.28, No.8, pp.1367-1372, Aug. 1989.

8 Y. Misaki, M. Mikawa, T. Ishiguro, and K. Hamasaki, "Effect of N2 partial pressure on the structure of MgO thin films deposited by radio frequencymagnetron sputtering with single-crystal MgO target", J. Vac. Sci. Technol., A 15(1), pp.48-51, Jan/Feb 1997.

9 S. Miki, Y. Uzawa, A. Kawakami, Z. Wang, and N. Kaya, "Fabrication and IF bandwidth measurement of NbN hot-electron bolometers", IEICE Technical Report, SCE99-25, 1999.

10 S. Miki, N. Kaya, Y. Uzawa, A. Kawakami, and Z. Wang, "NbN phonon-cooled hot-electron bolometers prepared on MgO substrate", Proc. Int. Superconductive Electronics Conference (ISEC'99), pp.453-455, Berkeley, CA, Jun. 1999.

11 A. Kawakami, S. Miki, and Z. Wang, "Epitaxial NbN/MgO/NbN Multilayers Using Reactive DC-Sputtering", The IEICE Transactions on Electronics (Japanese Edition), Vol.J84-C, No.4, pp.300-307, Apr. 2001.

12 A. Kawakami, Z. Wang and, S. Miki, "Low-loss epitaxial NbN/MgO/NbN trilayers for THz applications", IEEE Trans. Appl. Supercond., Vol.11, pp.80-83, Mar. 2001.

13 A. Kawakami and Z. Wang, "Fabrication and characterization of epitaxial NbN/MgO/NbN Josephson tunnel junctions", J. Appl. Phys., Vol.90, No.9, pp.4796-4799, Nov. 2001.

14 M. Maezawa, M. Aoyagi, H. Nakagawa, I. Kurosawa, and S. Takada, "Subgap characteristics of Nb/AlOx/Nb tunnel junctions with high current density", IEEE Trans. Appl. Supercond., Vol.5, pp.3073-3076, Jun. 1995.

15 A. W. Kleinsasser, W. H. Mallison, and R. E. Miller, "Nb/AlN/Nb Josephson junction with high critical current density", IEEE Trans. Appl. Supercond., Vol.5, pp.2318-2321, Jun. 1995.

16 A. Kawakami, Z. Wang, and B. Komiyama, "Measurements of Dielectric Constants and Surface Resistance for mm and submm Wavelength Region Using Josephson Effect", The IEICE Transactions on Electronics (Japanese Edition), Vol.J76-C-II, No.9, pp.593-600, 1993.

17 A. Kawakami, Z. Wang and, S. Miki, "Estimation of surface resistance for epitaxial NbN films in the frequency range of 0.1-1.1 THz", IEEE Trans. Appl. Supercond., Vol.13, pp.1147-1150, Jun. 2003.

18 J. Zmuidzinas, J. W. Kooi, J. Kawamura, G. Chattopadhyay, B. Bumble, H. G. LeDuc, and J. A. Stern, "Development of SIS mixers for 1 THz", Proc. SPIE, Vol.3357, pp.53-61, 1998.

19 A. Kawakami, Y. Uzawa, and Z. Wang, "Development of epitaxial NbN/MgO/NbN-SIS mixers for operations over the Nb gap frequency", Appl. Phys. Lett., Vol.83, No.19, pp.3954-3956, Nov. 2003.

20 Y. Uzawa, Z. Wang, and A. Kawakami, "Performance of quesi-optical mixer with NbN/AlN/NbN tunnel junctions and NbN tuning circuit at 760 GHz", Appl. Supercond., Vol.6, pp.465-475, 1998.

21 S. Miki, Y. Uzawa, A. Kawakami, and Z. Wang, "Fabrication and IF Bandwidth Measurement of NbN Hot-Electron Bolometers", The IEICE Transactions on Electronics (Japanese Edition), Vol.J83-C, No.9, pp.867-872, 2000.

KAWAKAMI Akira, *Ph.D.*

Senior Researcher, Nano ICT Group, Kobe Advanced ICT Research Center

Superconducting Electronics

TAKEDA Masanori, *Ph.D.*

Expert Researcher, Nano ICT Group, Kobe Advanced ICT Research Center

Superconducting Mixer Technology

WANG Zhen, *Ph.D.*

Group leader, Nano ICT Group, Kobe Advanced ICT Research Center

Superconductive Electronics